Supporting Information for

Terrestrial Water Storage Anomalies Emphasize Interannual Variations in Global Mean Sea Level During 1997–1998 and 2015–2016 El Niño Events

Yan-Ning Kuo[1], *Min-Hui Lo[1], Yu-Chiao Liang[2,3], Yu-Heng Tseng[4], Chia-Wei Hsu[5]

[1]Department of Atmospheric Sciences, National Taiwan University, Taipei, Taiwan

[2]Lamont-Doherty Earth Observatory, Columbia University, Palisades, NY, USA,

[3]Woods Hole Oceanographic Institution, Woods Hole, MA, USA,

[4]Institute of Oceanography National Taiwan University, Taipei, Taiwan

[5] Department of Atmospheric Science, Colorado State University, Colorado, USA

*corresponding author: Min-Hui Lo (minhuilo@ntu.edu.tw)

All the data used in this study are available online (see Acknowledgements and Data Availability Statement). The indices and variables are briefly described in Table S1.

Table S1. The indices and data used in this study

Dataset	Source/reference	Resolution	Time coverage in this study	Variable (variable names)
index	NOAA	Time series	1993–2016	Ocean Niño Index (ONI)
index	Website of Dr. Yu, Jin-Yi	Time series	1993–2016 (1981–2016 in SI)	Eastern Pacific Niño Index (EPI) and Central Pacific Niño Index (CPI)
Altimetry	AVISO	0.25°x0.25°	1993–2016	Sea level anomaly (SLA)
Argo	SIO	1°x1°	2004–2016	Salinity (S) and potential temperature (PT)
GRACE	JPL	0.5°x0.5°	2002–2016	Liquid water equivalent (LWE)
ECCOv4r4	JPL	0.5°x0.5°	1993–2016	Salinity (SALT), potential temperature (THETA), ocean bottom pressure with global mean air-pressure removed (OBPNOPAB)
ORAS5	ECMWF	1°x1°	1993–2016	Salinity (S), potential temperature (PT), Sea surface height (SSH)
ERA5-land	ECMWF	0.1°x0.1°	1993–2016 (1981–2016 in SI)	Total Precipitation (tp), Evapotranspiration (e), Runoff (ro)
RACMO2.3p2	Noël et al. (2018) and Van Wessem et al. (2018)	Antarctica (27km); Greenland (1km)	1993–2016	Surface water balance (SWB) of Greenland and Antarctica
CLM5	NCAR	0.9°x1.25°	1993–2016 (1981–2016 SI)	Atmospheric rain received from atmosphere (pre-repartitioning; RAIN_FROM_ATM), qflx_evap_soi + qflx_evap_can + qflx_tran_veg (QFLX_EVAP_TOT), total liquid runoff not including correction for land use change (QRUNOFF)

S1 Assimilation check for ECCOv4r4 with observations

Though the ocean model (MITgcm) used in ECCOv4r4 is a volume conserved model, for sea level budgets, the model developing team corrects the sea surface height field to make it comparable with observations by making three corrections: (1) the "Greatbatch correction", a time varying, globally-uniform correction to ocean volume due to changes in global mean density, (2) the inverted barometer

(IB) correction and (3) the "sea ice load" correction to account for the displacement of seawater due to submerged sea-ice and snow. In this study, we obtained the ocean bottom pressure without atmospheric pressure (OBPNOPAB), which was with above corrections to represent barystatic heights. Here we estimate the steric from the potential temperature and salinity.

Fig. S1a, S1c, and S1e show the maps of correlation coefficient between ECCOv4r4 and observational data for sea level anomaly (SLA), steric height, and barystatic height without removing linear trends and seasonal cycles. The correlation coefficients of SLA and steric height in tropical regions' grids are higher than in other regions while barystatic height is with more homogeneously distributed high correlation coefficients. Comparing with the three ocean basins, correlation coefficients of barystatic height in the Pacific Ocean are higher than the other two basins. Fig. S1b, S1d, S1f show the correlation maps of SLA, steric height and barystatic height with the linear trends and seasonal cycles being removed. For SLA and steric height, the correlation coefficients in tropical regions remain high but the correlation coefficients drop in mid-latitude after removing trends and seasonal cycles. For barystatic height, the correlation coefficients also decrease after removing trends and seasonal cycles but the spatial pattern is more homogeneous than the other two heights. Overall, although the correlation coefficients of ECCOv4r4 data and observational data decline after removing the linear trend and seasonal cycle, the correlation coefficients are still high with 95% confidence level in most of grid points.

Fig.S2 shows the comparison of global mean sea level (GMSL) heights from ECCOv4r4 and observations: AVISO for total sea level, Argo for steric and GRACE for barystatic height. The first column in Fig. S2 shows the SLA, steric height and barystatic height time series without removing linear trends and seasonal cycles. The second column in Fig. S2 shows the time series with linear trends and seasonal cycles removed. Figure S2 shows that ECCOv4r4 represents the observational sea level well, no matter for the total, steric or barystatic heights. However, after removing the trends and seasonal cycles, the correlation coefficients of the three heights drop, especially for steric height. The correlation coefficient of blue and red lines in Figure S2a – S2f are in Table S2 and all of them passed the student's t test for correlation coefficient, which indicates the interannual variations of sea level are well-captured by ECCOv4r4. Therefore, the data assimilated temperature and salinity fields have been incorporated into our estimation.

Previous studies also showed that the ocean reanalysis dataset was superior to free-running ocean model simulations in reproducing altimetry-derived trends. For example, Köhl et al. (2007) showed that unrealistic trends in ocean simulations, especially at high latitudes, are rectified in the ocean reanalysis, where data assimilation modifies the steric sea level variations and, to a lesser extent, the mass-induced variations. In summary, reanalysis datasets have shown an accuracy in capturing sea level variability at least comparable (if not superior) to observational or model-only products. Though it is undeniable that those corrections might produce artificial errors, ECCOv4r4 is the ocean reanalysis providing those sea level budgets we discussed and is commonly used for sea-level studies in the past (Storto et al., 2019; Piecuch and Ponte, 2011).

S2 Estimating the uncertainty of the difference of peaks in the two events

The uncertainty here for the difference of peaks in the two events was calculated using the standard deviation obtained from applying an AR(3) model (autoregression model based on 3 earlier time steps):

$$y(t) = a_1 y(t-1) + a_2 y(t-2) + a_2 y(t-3) + \varepsilon(t)$$

where $\varepsilon(t)$ is a random noise with a prescribed variance as:

$$\sigma_\varepsilon^2 = R_0 - \sum_{k=1}^{3} a_k R_k$$

The coefficients (a_1 – a_3) in AR model are determined using the Yule-Walker algorithm, based on the one-sided autocovariance (negative lags are assumed to be the same as positive lags in the computation:

$$\begin{pmatrix} a_1 \\ a_2 \\ a_3 \end{pmatrix} = \begin{pmatrix} R_0 & R_1 & R_2 \\ R_1 & R_0 & R_1 \\ R_2 & R_1 & R_0 \end{pmatrix}^{-1} \begin{pmatrix} R_1 \\ R_2 \\ R_3 \end{pmatrix}$$

R_0 – R_3 are autocovariance at lag=0–lag=3. We used the means and standard deviations of $y(t)$ (anomalies of GMSL, -TWS in the main text) and their corresponding $\varepsilon(t)$ to make random sampling and perform 10,000 Monte Carlo simulations based on the AR model.

Because the time series are highly autocorrelated, we considered the effective sample size (*ESS*) when calculating the t score:

$$ESS = N \times \frac{1 - r_y}{1 + r_y}$$

Here, *N* is the length of the data (288 for monthly data during 1993–2016), r_y is the lag-1 autocorrelation correlation coefficient of *y*. Finally, the uncertainty of the

difference of the two peaks in each event is calculated as the 90% confidence interval based on the standard deviation (σ_{MC}) of the mean of those 10,000 Monte Carlo simulated time series:

$$Peak\ difference \pm t_{95} \cdot \sigma_{MC}$$

S3 Significance test for correlation coefficient

The ENSO and the variables discussed in this study may have persistence manifested as high autocorrelation. Therefore, we considered the effective sample size (Bretherton et al. 1999) when performing statistical significance test of correlation coefficients for two time series. The *ESS* is calculated as:

$$ESS = N \times \frac{1 - r_{index} r_{variable}}{1 + r_{index} r_{variable}}$$

Where *N* is the length of the data (e.g. in Fig. 3, is 288 for monthly data during 1993-2016), r_{index} is the lag-1 autocorrelation correlation coefficient of the ENSO index and $r_{variable}$ is the lag-1 autocorrelation correlation coefficient of variable of interest (e.g. GMSL, -TWS, etc).

The Student's t-score is calculated as:

$$t = r \times \sqrt{\frac{ESS - 2}{1 - r^2}}$$

Where *r* is the correlation coefficient between index and variable of interest.

S4 Significance test and the 90% confidence interval for regression slope

The ordinary least squares (OLS) linear regression is applied for the calculation of regression slope (β_1):

$$y = \hat{y} + \epsilon$$
$$\hat{y} = \beta_1 x + \beta_0$$

Where *x* is the predictor variable (here CPI or EPI), *y* is the criterion variable (here TWS), $\hat{y}$ is the predicted y by the regression model, β_1 is the regression slope, β_0 is the intercept, and ϵ is the residual as $y - \hat{y}$.

The F-statistic for testing the regression slope is calculated as:

$$F = \frac{MSR}{MSE}$$

Following

$$MSR = \frac{\sum(\hat{y}_i - \bar{y})^2}{1}$$

$$MSE = \frac{\sum(y_i - \hat{y}_i)^2}{ESS - 2}$$

$$ESS = N \times \frac{1 - r_\epsilon}{1 + r_\epsilon}$$

MSR is the regression mean square, *MSE* is the mean square error. Because ϵ is also highly autocorrelated, we accounted for the *ESS* of the ϵ as well. Here, *N* is the length of the data (e.g. in Fig. 3, is 288 for monthly data during 1993–2016), r_ϵ is the lag-1 autocorrelation correlation coefficient of the residual.

The uncertainty of the regression slope in Table 1 is calculated as the 90% confidence interval (Piecuch and Quinn, 2016):

$$\beta_1 - t_{95} \cdot \sigma \leq \beta_1 \leq \beta_1 + t_{95} \cdot \sigma$$

Where the standard error (σ) is

$$\sigma = \sqrt{\frac{\epsilon^T \epsilon}{ESS - 2} (x^T x)^{-1}}$$

Figure S1. (a) Correlation map of sea level anomaly between AVISO+ and steric-plus-barystatic in ECCOv4r4 (1993–2016, with linear trend and the seasonal cycle), (b) Correlation map of sea level anomaly between AVISO+ and steric-plus-barystatic in ECCOv4r4 (1993–2016, linear trend and the seasonal cycle are removed), (c) as (a) but for steric between Argo and ECCOv4r4 (2004–2016, with linear trend and the seasonal cycle), (d) as (b) but for steric between Argo and ECCOv4r4 (2004–2016, linear trend and the seasonal cycle are removed), (e) as (a) but for barystatic between GRACE and ECCOv4r4 (2003–2016, with linear trend and the seasonal cycle), (f) as (b) but for barystatic between GRACE and ECCOv4r4 (2003–2016, linear trend and the seasonal cycle are removed). Only the grids whose correlation coefficient is with 95% confidence level are shown with colors in these figures.

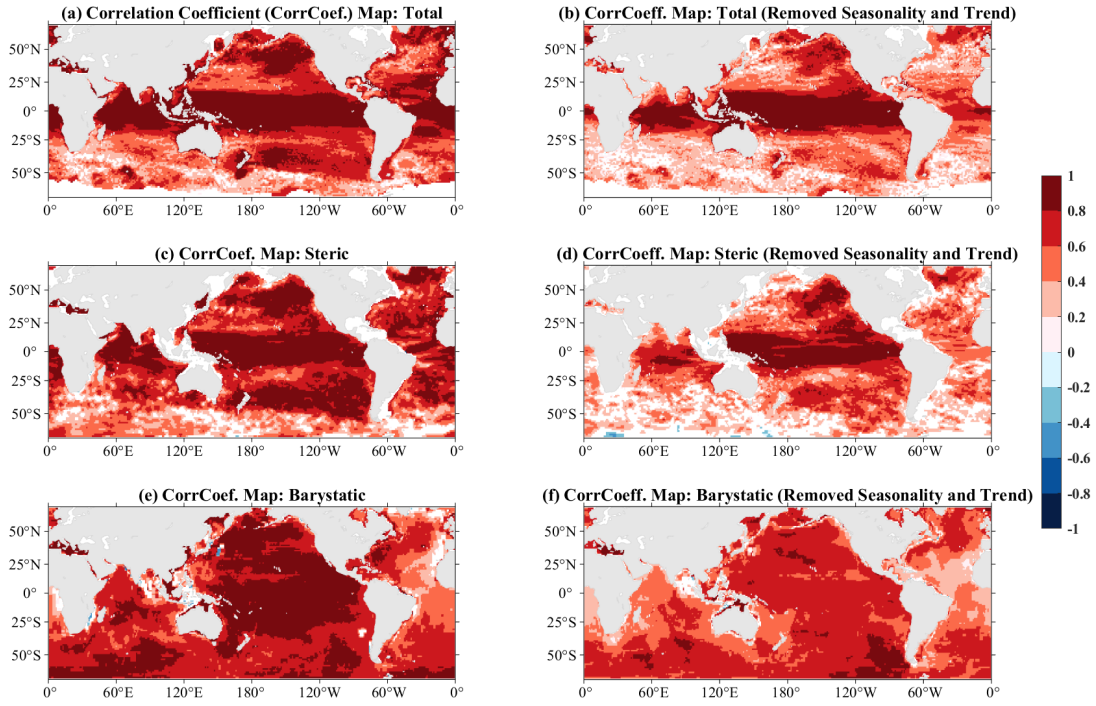

Figure S2. Time series of data from observation (-TWS from GRACE for barystatic height and Argo derived steric height) and ECCOv4r4. (a) GMSL, (b) GMSL that the linear trend and the seasonal cycle are removed, (c) steric height, (d) steric that the linear trend and the seasonal cycle are removed, (e) barystatic, (f) barystatic that the linear trend and the seasonal cycle are removed.

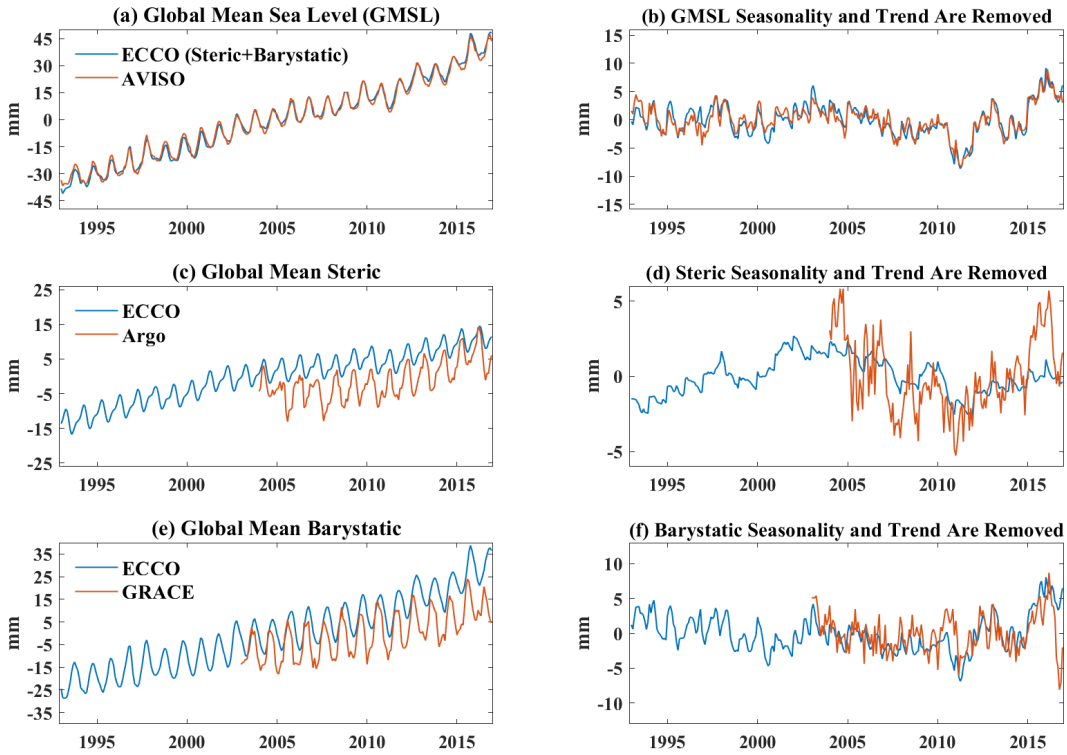

Table S2. Correlation Coefficient of red and blue lines in Figure S2 that with p<0.01 and effective sample size being considered.

Figure S2	Correlation Coefficient
(a)	1.00
(b)	0.91
(c)	0.92
(d)	0.56
(e)	0.80
(f)	0.50

Figure S3. As Figure 3 but using TWS data from CLM5 simulation. Mean TWS during (a) July 1997 – June 1998 and (b) July 2015 – June 2016. (c) The difference from (b) minus (a). The numbers at the lower left corners Fig. 3a–3c are the global area-weighted mean -TWS contributing to GMSL in each figure. Regression maps of (d) TWS and EP indices during 1993–2016, (e) TWS and CP indices during 1993–2016. Boxed regions are discussed in text and dotted grids passed the F-test with p-value < 0.05 for the regression slope.

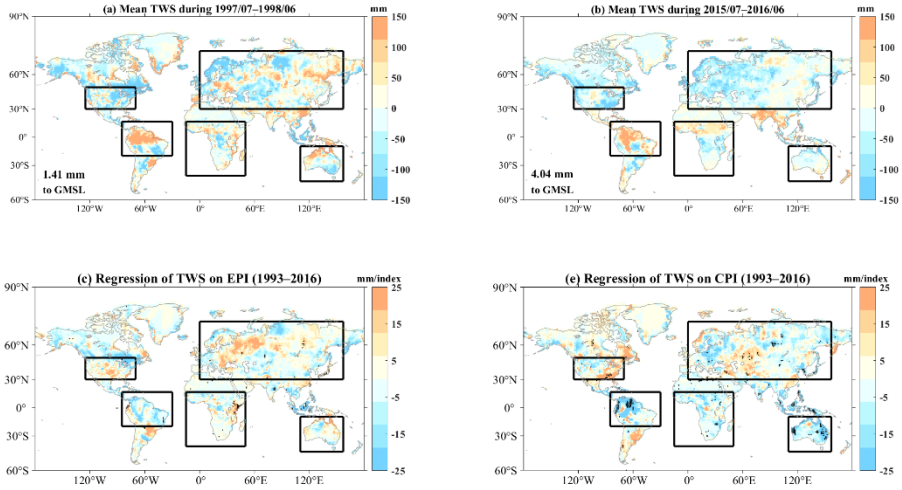

Figure S4. Regression maps of (a) TWS (ERA5-land) and EP indices during 1981–2016, (b) TWS (ERA5-land) and CP indices during 1981–2016, (c) TWS (CLM5) and EP indices during 1981–2016, and (d) TWS (CLM5) and CP indices during 1981–2016.

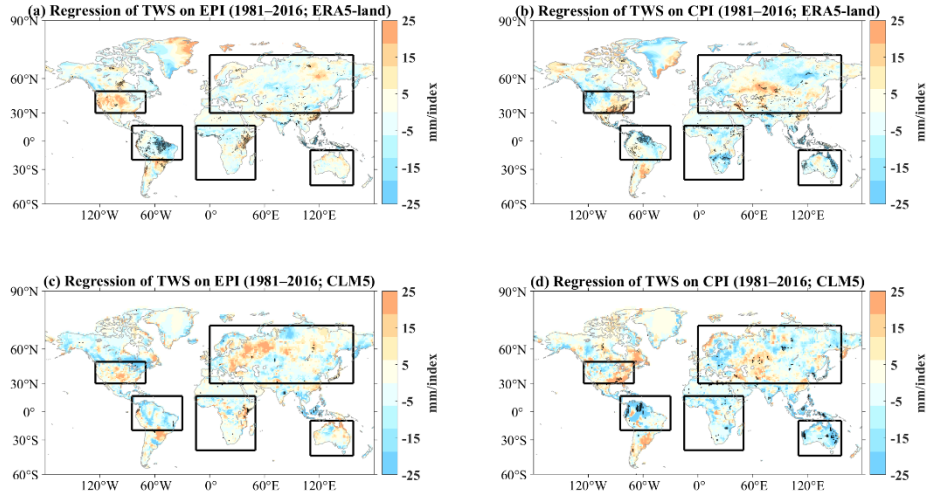

S5 Results from ORAS5

A brief comparison of ECCOv4r4 and ORAS5 in terms of the linear trends, magnitudes of sea level variation are shown in Table S4. The barystatic from ORAS5 is derived from the subtraction of SSH and steric sea level. The total sea level in ORAS5 is assimilated with sea level observation from satellite altimetry; however, we should note that the steric trend in ORAS5 is higher than ECCOv4r4's. The steric trends is reported to be higher in ORAS5 than other reanalysis data and it might come from the overall higher temperature and salinity trends (Carton et al., 2019; Storto et al., 2019).

Table S3. The values of linear trends with standard error calculated with 90% confidence level; standard deviations of each time series are calculated with seasonal cycle and trend removed. (Calculated from ECCOv4r4 and ORAS5).

	ECCOv4r4					
	Linear trend (unit: mm/year)			Standard deviation (unit: mm)		
	Total	Steric	Barystatic	Total	Steric	Barystatic
Global	3.07±0.001	0.96±0.001	2.11±0.001	2.74	1.22	2.62
	ORAS5					
	Linear trend (unit: mm/year)			Standard deviation (unit: mm)		
	Total	Steric	Barystatic	Total	Steric	Barystatic
Global	3.10±0.001	2.31±0.002	0.79±0.003	3.31	4.41	6.23

* Note that uncertainty of trends here are calculated depending on the standard error of linear regression. The uncertainty in knowing systematic drifts of ±0.6mm/year in GMSL and the uncertainty in GIA of ±0.3mm/year mentioned in Chambers et al. (2017) are excluded.

Figure S5 As Fig. 1b, c but from ORAS5. The steric heights of ORAS5 are derived following Gill and Niller (1973) and the barystatic height of ORAS5 is calculated as sea surface height subtracting steric height.

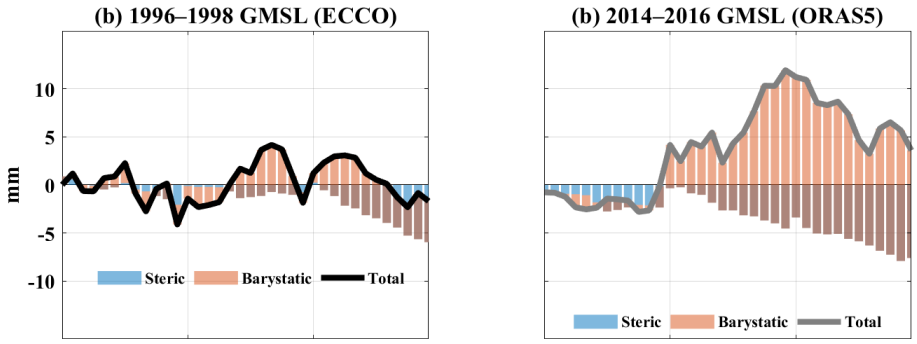

Figure S6. Time series of global mean sea level (GMSL) contributed from barystatic height from ECCOv4r4 (purple line), GMSL contributed from global mean -TWS from GRACE (green line), GMSL contributed from global mean -TWS from ERA5-Land (yellow line), GMSL contributed from global mean -TWS from CLM5 (red line), and GMSL contributed from barystatic height from ORAS5 (blue line). Gray-shaded areas are for 1996–1998 and 2014–2016 events.

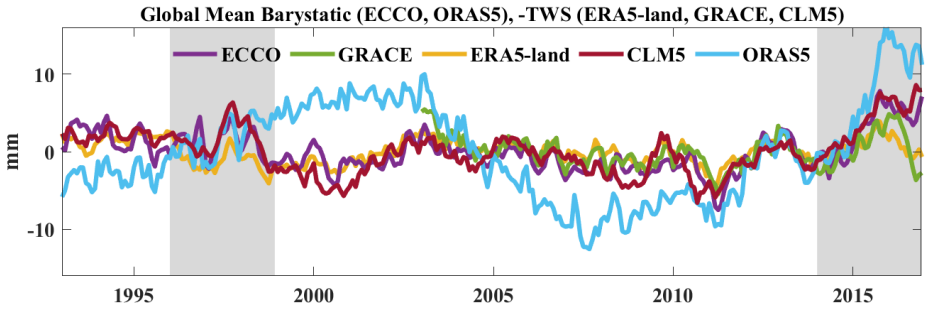

Reference:

Bretherton, C. S., M. Widmann, V. P. Dymnikov, J. M. Wallace, and I. Bladé, 1999: The effective number of spatial degrees of freedom of a time-varying field. *J. Climate*, 12, 1990–2009, https://doi.org/10.1175/15200442(1999)012,1990:TENOSD.2.0.CO;2.

Carton, J. A., Penny, S. G., & Kalnay, E. (2019). Temperature and salinity variability in the SODA3, ECCO4r3, and ORAS5 ocean reanalyses, 1993–2015. *Journal of Climate*, *32*(8), 2277-2293.

Chambers, D. P., Cazenave, A., Champollion, N., Dieng, H., Llovel, W., Forsberg, R., ... & Wada, Y. (2017). Evaluation of the global mean sea level budget between 1993 and 2014. *Surveys in Geophysics*, *38*(1), 309-327.

Köhl, A., Stammer, D., & Cornuelle, B. (2007). Interannual to decadal changes in the ECCO global synthesis. Journal of Physical Oceanography, 37(2), 313-337.

Noël, B., van de Berg, W. J., Van Wessem, J. M., Van Meijgaard, E., Van As, D., Lenaerts, J., ... & Van De Wal, R. S. (2018). Modelling the climate and surface mass balance of polar ice sheets using RACMO2-Part 1: Greenland (1958-2016). *Cryosphere*, *12*(3), 811-831.

Piecuch, C. G., & Ponte, R. M. (2011). Mechanisms of interannual steric sea level variability. *Geophysical Research Letters*, *38*(15).

Piecuch, C. G., & Quinn, K. J. (2016). El Niño, La Niña, and the global sea level budget. *Ocean Science*, *12*(6), 1165-1177.

Storto, A., Bonaduce, A., Feng, X., & Yang, C. (2019). Steric sea level changes from ocean reanalyses at global and regional scales. Water, 11(10), 1987.

Van Wessem, J. M., Jan Van De Berg, W., Noël, B. P., Van Meijgaard, E., Amory, C., Birnbaum, G., ... & Ligtenberg, S. R. (2018). Modelling the climate and surface mass balance of polar ice sheets using racmo2: Part 2: Antarctica (1979-2016). *Cryosphere*, *12*(4), 1479-1498.